The 2011 off the Pacific coast of Tohoku Earthquake related to a strong velocity gradient with the Pacific plate

Makoto Matsubara[1] and Kazushige Obara[2]

[1]*National Research Institute for Earth Science and Disaster Prevention, Tsukuba, Japan*
[2]*Earthquake Research Institute, the University of Tokyo, Tokyo, Japan*

(Received April 10, 2011; Revised May 15, 2011; Accepted May 18, 2011; Online published September 27, 2011)

We conduct seismic tomography using arrival time data picked by NIED Hi-net, including earthquakes off the coast, outside the seismic network. For these offshore events, we use the NIED F-net focal depth. We detect two low-V zones in the uppermost subducting oceanic crust. The landward low-V zone with a large anomaly corresponds to the western edge of the coseismic slip zone of the 2011 off the Pacific coast of Tohoku Earthquake. The asperities of the previously known Off-Miyagi and Off-Fukushima earthquakes with magnitudes around 7.0 are also located at the boundary of the low-V and the eastern high-V zones. The initial break point (hypocenter) is associated with the edge of a slightly low-V and low-V_p/V_s zone. The trenchward low-V and low-V_p/V_s zone extending southwestward from the hypocenter may indicate the existence of a subducted seamount. The high-V zone and low-V_p/V_s zone might have accumulated the strain and resulted in the huge coseismic slip zone of the 2011 Tohoku Earthquake. The low-V and low-V_p/V_s zone is a slight fluctuation within the high-V zone and might have acted as the initial break point of the 2011 Tohoku Earthquake.

Key words: Seismic tomography, the 2011 off the Pacific coast of Tohoku Earthquake, high-V coseismic slip zone, seamount, NIED Hi-net, NIED F-net, low-V oceanic crust, asperity.

1. Introduction

The 2011 off the Pacific coast of Tohoku Earthquake occurred on March 11, 2011. There are few studies (e.g. Zhao *et al*., 2007) of the velocity structure near the Japan trench using data from inland seismic stations. It is difficult to investigate the velocity structure beneath the ocean with only the inland seismic stations because of the large uncertainty in earthquake focal depth outside of the seismic network. Zhao *et al*. (2007) estimated the velocity structure near the Japan trench using the focal depths constrained by *sP* converted waves. The broadband seismograph network (F-net) operated by National Research Institute for Earth Science and Disaster Prevention (NIED) determines the focal depths of events with magnitudes larger than 3.5 using a Green's function approach (Okada *et al*., 2004). For the events distant from the seismic network, the depth determined by NIED F-net is more reliable than that determined by the high sensitivity seismograph network (Hi-net) operated by NIED, since there are no stations above the hypocenter. However, NIED determines reliable arrival times from those events at onshore stations. To use those data effectively, we combined the arrival time data picked by NIED Hi-net and the focal depth determined by NIED F-net. By using the distant events off the coast, we can obtain the velocity structure of the lower crust, the upper mantle, and the plate boundary from the trench to the island arc.

2. Data, Method, Resolution, and Comparison with the Results of OBS

The target region, 20–48°N and 120–148°E, covers the Japanese Islands from Hokkaido to Okinawa. Matsubara *et al*. (2008) used only the earthquakes at depths of 0–200 km within 50 km of Hi-net stations and some events at depths of 200–425 km outside of the network. In the present study, we use the events off the coast whose focal depths are determined by NIED F-net. The depths of the events off the coast are not well determined with only the stations in land. NIED F-net determines moment tensor solutions using long-period (20–50 s) waves by comparing the Green's function database calculated with intervals of 3 in depth and 5 km in the horizontal direction (Fukuyama *et al*., 1998) using a layered 1-D velocity structure. Sometimes the NIED Hi-net system determines the depths of offshore earthquakes deeper than the true depths because of the lack of stations above the hypocenters and traveltime data of P- and S-waves observed at stations distributed only on the west side of the hypocenters. Those events are located deeper as they get close to the trench in spite of the plate boundary becoming shallower. Earthquakes with low-angle thrust focal mechanism determined by NIED F-net tend to get shallower close to the trench along the subducting Pacific plate. We fix the depth of those events as determined by NIED F-net. We conduct seismic tomography with those data and relocate only the horizontal location in the inversion. A total of manually picked 4,622,346 P-wave and 3,062,846 S-wave arrival times for 100,733 earthquakes

doi:10.5047/eps.2011.05.018

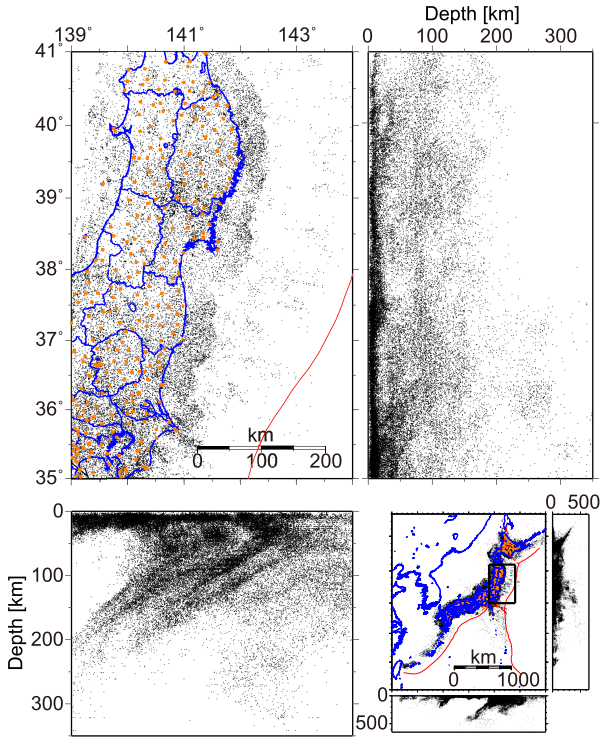

Fig. 1. Distribution of hypocenters and seismic stations used in this study. Black dots and brown crosses denote the hypocenters and seismic stations, respectively. Blue lines denote the coastline and prefecture boundaries. Red lines show the plate boundaries at the surface.

Table 1. Grid interval and resolution size.

Depth	Grid interval		Resolution/Checkerboard pattern	
	Horizontal	Vertical	Horizontal	Vertical
0–10	0.1°	2.5 km	0.2°	5 km
10–40		5 km		10 km
40–60		10 km		20 km
60–180		15 km		30 km
180–300		20 km		40 km
300–		25 km		50 km

recorded at 1,212 stations (Fig. 1) from October 2000 to August 2009 are available for use in the tomographic method. These stations are maintained by multiple organizations including NIED, the Japan Meteorological Agency (JMA), and universities. The details of this method are explained in Matsubara *et al*. (2004, 2005). The data set consists of manually picked data; NIED picks the arrival time at stations as distant from the epicenter as possible.

We follow the technique of Matsubara *et al*. (2004, 2005), who introduced spatial velocity correlation and station corrections to the original code of Zhao *et al*. (1992). Grid nodes were placed with a separation smaller than the spatial resolution, with smoothing performed in order to stabilize the solution. The inverse problem is then solved with the LSQR algorithm (Nolet, 1987) since we can assume arbitrary damping matrix with a combination of diagonal and smoothing matrices.

We employ a 3D grid net to construct the velocity (slowness) structure. The grid spacing is shown in Table 1. The 1D structure used in the routine determination of hypocenters at NIED (Ukawa *et al*., 1984) is used as the initial model. We do not impose velocity discontinuities in this study since incorrect configuration of the boundaries would lead to an incorrect solution.

We solve for the location and origin time of all the earthquakes as well as the P and S-wave slowness at each grid point with more than 10 associated rays. In the final iteration, we estimate the P-wave slowness at 458,234 nodes and the S-wave slowness at 347,037 nodes. The inversion reduces the root mean square of the P-wave traveltime residual from 0.455 s to 0.187 s and that of the S-wave data from 0.692 s to 0.228 s after eight iterations.

We conduct a checkerboard resolution test in order to evaluate the reliability of the obtained solution. We assumed a $\pm 5\%$ checkerboard pattern and calculated synthetic traveltimes with random noise of zero mean and standard deviations of 0.05 s and 0.1 s for P- and S-waves, respectively, derived from the estimated uncertainty of the arrival times. Figure 2(a) shows the result of the checkerboard resolution test at a depth of 30 km. We identify the well-resolved region numerically with consideration of the recovery rate and stability of the solution of the checkerboard test using the same method as Matsubara *et al*. (2004, 2005, 2008, 2009) and show the results in color where good resolution is obtained as Fig. 2(b) hereafter.

The results of the velocity/perturbation structures within the Pacific plate and vertical cross sections are represented (Figs. 3 and 4). The velocity perturbation is relative to the averaged velocity at each depth. We compare the vertical cross section of the velocity structure off-Fukushima (Fig. 4(e)) and off-Miyagi (Fig. 4(b)) with those derived from the OBS observations (Miura *et al*., 2003, 2005). The high-V uppermost mantle at the depths of 30–50 km as the mantle wedge zone is consistent with the results from OBS analysis (Fig. 4(e)) off Fukushima. This result supports the reliability of the current study.

3. Result

We determine the upper boundary of the Pacific plate based on the velocity structure and earthquake hypocentral distribution. The upper boundary of the low-V oceanic crust corresponds to the plate boundary where thrust earthquakes are expected to occur. Where we don't observe low-V oceanic crust, we determine the upper boundary of the upper layer of the double seismic zone within the high-V Pacific plate. We assume the depth at the Japan trench as 7 km.

Figure 3 shows the map view of V_P perturbation within the Pacific plate 10 km beneath the boundary. In the inland area, large earthquakes occurred around the region whose lower crust has low-V, suggesting a role of magma and fluid (Zhao *et al*., 2010). Then we investigate the velocity structure within the Pacific plate such as 10 km beneath the plate boundary.

We detected two low-V zones in the oceanic crust at the uppermost part of the Pacific plate on the west side of the hypocenter (Fig. 3). We define one of them at longitudes of approximately 142.5E adjacent to the hypocenter as the trenchward low-V zone and another at longitudes of 141.5–142.0E as the landward low-V zone. We also call

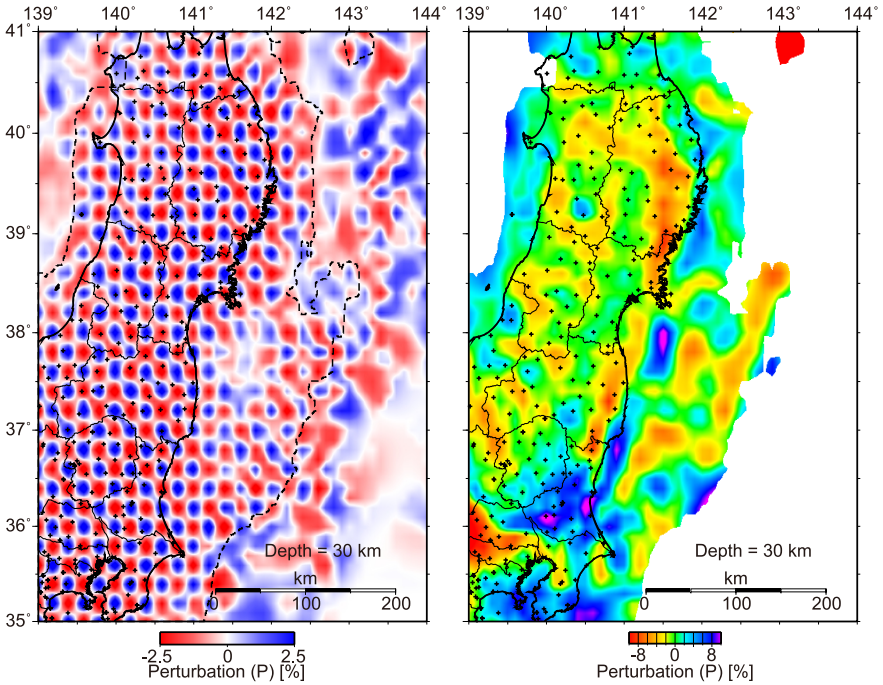

Fig. 2. Result of checkerboard resolution test and P-wave velocity perturbation at a depth of 30 km. Black broken lines surround the resolved zone.

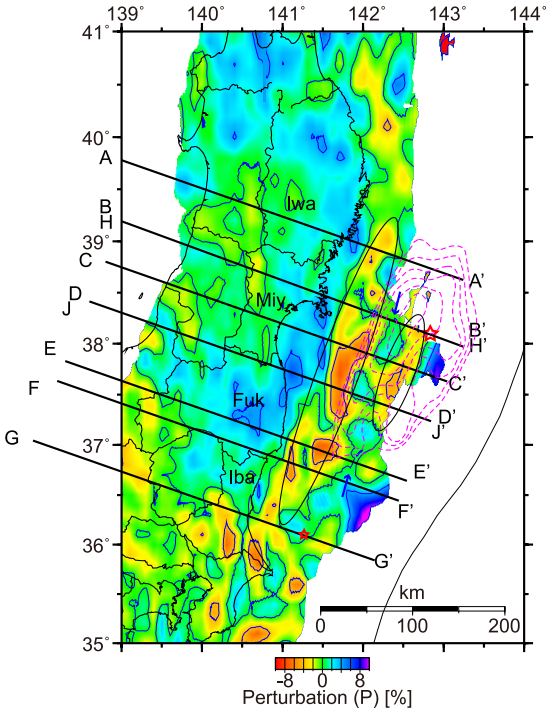

Fig. 3. Map view of P-wave velocity perturbation within the Pacific plate 10 km beneath the upper boundary of the Pacific plate. Red star on B–B′=H–H′ shows the location of the hypocenter of the 2011 Tohoku Earthquake. Small red star on G–G′ denotes the hypocenter of the aftershock off Ibaraki. Large and small ellipses show the location of landward and trenchward low-V zones, respectively. Blue arrows between the ellipses denote the central high-V zone. Purple broken contours show the area of strong energy radiation estimated with MeSO-net data (Honda *et al*., 2011). Thin black line shows the Japan trench. Black lines denote the location of cross sections in Fig. 4. Iwa: Iwate, Miy: Miyagi, Fuk: Fukushima, Iba: Ibaraki prefecture.

the high-V zone between them the 'central high-V zone.' The landward low-V zone extends broadly and has large anomaly; however, the trenchward low-V zone has slight anomaly and is a small fluctuation within the high-V zone. The hypocenter of the 2011 Tohoku Earthquake is located at the northern edge of the resolved zone; however, the structure on the southern side of the hypocenter shows that the hypocenter is located at the boundary of the trenchward slightly low-V and eastern high-V zone.

The vertical cross sections along the direction of the subducting Pacific plate are shown in Fig. 4. The low-V oceanic crust at the uppermost part of the Pacific plate is imaged extending downdip from the hypocentral region and diminishes beneath the land area (Fig. 4(a)–4(e)). The trenchward low-V zone near the Japan trench is imaged off Iwate, Miyagi, and Fukushima and corresponds to the oceanic crust of the Pacific plate (Fig. 4(a)–4(e)); however, there is no clear low-V oceanic crust off the boundary of Fukushima and Ibaraki near the Japan trench (Fig. 4(f)). We only observe low-V oceanic crust at the uppermost part of the Pacific plate at depths of 40–60 km within the landward low-V zone.

4. Discussion

The high-V region on the east side of the hypocenter and the central high-V region between the two low-V zones are covered with the coseismic slip regions estimated using GPS data (Geospatial Information Authority, 2011) or waveform data (e.g. Yagi, 2011; Shao *et al*., 2011). Honda *et al*. (2011) estimate a rupture of the earthquake with the seismic network in the metropolitan area (MeSO-net). The area of strong energy radiation is located at the west side of the hypocenter offshore of Miyagi and extends eastward and southward. The area of the strongest energy radiation is consistent with the central high-V zone between the trench-

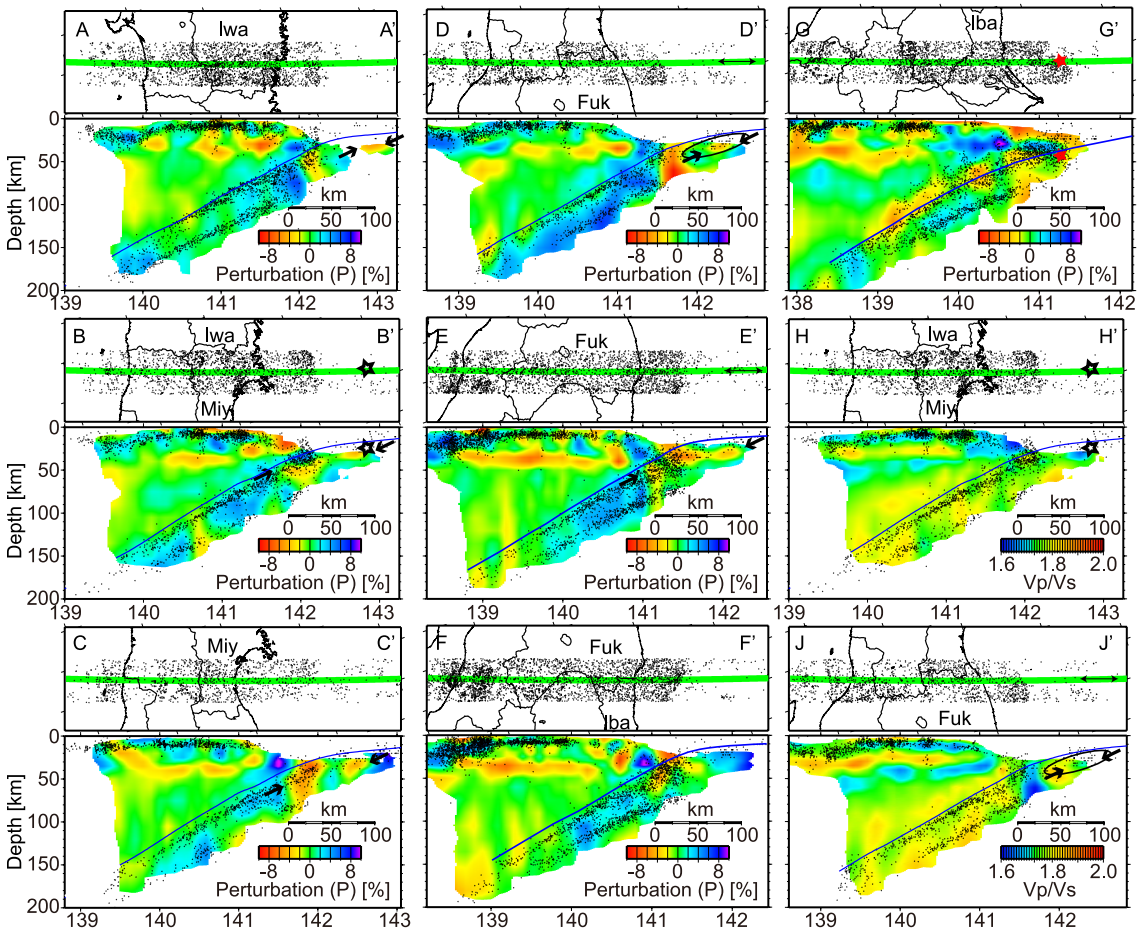

Fig. 4. WNW-ESE vertical cross sections of V_p perturbation and V_p/V_s beneath the Tohoku region. Black dots denote the hypocenters used for seismic tomography within 20 km of the cross section. Blue lines show the upper boundary of the Pacific plate. Large stars in B–B′ and H–H′ show the hypocenter of the 2011 Tohoku Earthquake determined by JMA. Small star in G–G′ denotes the hypocenter of the aftershock off Ibaraki. Circle in D–D′ corresponds to the relatively large slip zone estimated by Honda *et al*. (2011). Arrows in the upper panels of D–D′ and E–E′ denote the location of convex configuration of seafloor found. Arrows in the lower panels of A–A′ to E–E′ show the low-V oceanic crust.

ward and landward low-V zones (Fig. 3). The landward low-V zone is located at the western boundary of the zone of strong energy radiation. The asperities of the preknown Off-Miyagi and Off-Fukushima earthquakes with magnitude around 7.0 (Sato *et al*., 1989) are also located at the boundary of the landward low-V zone and the central high-V zone.

The initial break point (hypocenter) of the 2011 Tohoku Earthquake is located at the boundary of the trenchward slightly low-V and high-V zone (Fig. 3). There are some seamount chains offshore Fukushima and Ibaraki (Yamasaki and Okamura, 1989). A convex seafloor configuration may indicate the existence of subducted seamounts beneath the cross sections D–D′ and E–E′ (Hudnut, 2011) corresponding to the trenchward low-V zone. In terms of E–E′, there is a convex undulation at the plate boundary imaged by refraction seismology (Miura *et al*., 2003). The trenchward low-V region on the west side of the hypocenter has low-V_p/V_s (Fig. 4(h), 4(j)). We propose that fluid with high aspect ratio pores exists there, as proposed by Matsubara *et al*. (2004, 2009) based on the result of Takei (2002). Nakamichi *et al*. (2007) and Kato *et al*. (2010) also considered the high aspect ratio crack with low-V_p/V_s zone. If a large seamount has already subducted beneath the plate, a low-V zone would be imaged (Cummins *et al*., 2002). The low-V and low-V_p/V_s zone beneath D–D′ may indicate the subducted seamount. This trenchward low-V_p/V_s zone extends to the initial break point of the mainshock (B–B′).

The area of strong energy radiation also extends to the high-V zone on the east side of the hypocenter (Fig. 3). The high-V zone on the east side of the landward low-V zone and low-V_p/V_s zone might have accumulated the strain and resulted in the huge coseismic slip zone of the 2011 Tohoku Earthquake. The trenchward low-V and low-V_p/V_s zone is a slight fluctuation within the high-V zone and might have acted as the initial break point of the 2011 Tohoku Earthquake.

Beneath the southern Ibaraki prefecture, the low-V oceanic crust of the Pacific plate is clearly imaged at depths of 40–130 km (Fig. 4(g)), which is consistent with previous studies (e.g. Matsubara *et al*., 2005; Shelly *et al*., 2006). Matsubara *et al*. (2005) proposed that the subducting Philippine Sea plate distorts the corner flow induced by the Pacific plate and suppresses thermal recovery in the mantle wedge. There is a large aftershock with magnitude 7.7 off southern Ibaraki half an hour after the 2011 Tohoku Earthquake. The hypocenter is also located at the boundary of the eastern

low- and western high-V zones.

5. Conclusion

We combine the NIED F-net hypocentral and Hi-net arrival time data and apply seismic tomography to estimate the seismic velocity structure outside of the network. We obtain the horizontal 20-km and vertical 10-km scale structure near the Japan trench. There are two low-V zones within the subducting oceanic crust. The landward low-V zone with a large anomaly is consistent with the western edge of the coseismic slip zone of the 2011 off the Pacific coast of Tohoku Earthquake. The asperities of the previously known Off-Miyagi and Off-Fukushima earthquakes with magnitudes around 7.0 are also located at the boundary of the landward low-V zone and the central high-V zone. The zone beneath the initial break point of the 2011 Tohoku Earthquake is associated with the edge of the slightly low-V and low-V_p/V_s zone corresponding to the boundary of the low- and high-V zone. The trenchward low-V and low-V_p/V_s materials extending to the southwest from the hypocenter may indicate a subducted seamount. The high-V zone on the east side of the landward low-V zone and low-V_p/V_s zone might have accumulated the strain and resulted in the huge coseismic slip zone of the 2011 Tohoku Earthquake. The low-V and low-V_p/V_s zone is a slight fluctuation within the high-V zone and might have acted as the initial break point of the 2011 Tohoku Earthquake.

Acknowledgments. We used the seismic data provided by the National Research Institute for Earth Science and Disaster Prevention, the Japan Meteorological Agency, Hokkaido University, Hirosaki University, Tohoku University, the University of Tokyo, Nagoya University, Kyoto University, Kochi University, Kyushu University, Kagoshima University, the National Institute of Advanced Industrial Science and Technology, the Geographical Survey Institute, Tokyo Metropolis, Shizuoka Prefecture, the Hot Springs Research Institute of Kanagawa Prefecture, Yokohama City, and the Japan Agency for Marine-Earth Science and Technology. We are very grateful to David Shelly for kindly discussing and improving our paper. We also thank William Ellsworth for the kind discussion and suggestions. We appreciate the many suggestions from the two anonymous reviewers. This study was supported by the project on the Operation of Seismograph Networks for the NIED. Some of the figures were drawn using Generic Mapping Tools software (Wessel and Smith, 1995) and the software for viewing 3D velocity structures beneath whole Japanese Islands (Matsubara, 2010).

References

Cummins, P. R., T. Baba, S. Kodaira, and Y. Kaneda, The 1946 Nankai earthquake and segmentation of the Nankai Trough, *Phys. Earth Planet. Inter.*, **132**, 75–87, 2002.

Fukuyama, E., M. Ishida, D. S. Dreger, and H. Kawai, Automated seismic moment tensor determination by using on-line broadband seismic waveforms, *Zisin (J. Seismol. Soc. Jpn.)*, **51**, 149–156, 1998 (in Japanese with English abstract).

Geospatial Information Authority, Coseismic slip distribution model inferred from GEONET data, http://www.gsi.go.jp/cais/topic110315-index-e.html, 2011.

Honda, R., Y. Yukutake, H. Ito, M. Harada, T. Aketagawa, A. Yoshida, S. Sakai, S. Nakagawa, N. Hirata, K. Obara, and H. Kimura, A complex rupture image of the 2011 off the Pacific coast of Tohoku Earthquake revealed by the MeSO-net, *Earth Planets Space*, **63**, this issue, 583–588, 2011.

Hudnut, K., Deep bank subduction in the 2011 Tohoku earthquake?, *Earth Planets Space*, 2011 (submitted).

Kato, A., T. Iidaka, R. Ikuta, Y. Yoshida, K. Katsumata, T. Iwasaki, S. Sakai, C. Thurber, N. Tsumura, K. Yamaoka, T. Watanabe, T. Kunitomo, F. Yamazaki, M. Okubo, S. Suzuki, and N. Hirata, Variations of fluid pressure within the subducting oceanic crust and slow earthquakes, *Geophys. Res. Lett.*, **37**, L14310, doi:10.1029/2010GL043723, 2010.

Matsubara, M., Software for viewing 3D velocity structures beneath whole Japan islands, *Report of the National Research Institute for Earth Science and Disaster Prevention*, **76**, 1–9, 2010.

Matsubara, M., N. Hirata, H. Sato, and S. Sakai, Lower crustal fluid distribution in the northeastern Japan arc revealed by high resolution 3D seismic tomography, *Tectonophysics*, **388**, 33–45, doi:10.1016/j.tecto.2004.07.046, 2004.

Matsubara, M., H. Hayashi, K. Obara, and K. Kasahara, Low-velocity oceanic crust at the top of the Philippine Sea and Pacific plates beneath the Kanto region, central Japan, imaged by seismic tomography, *J. Geophys. Res.*, **110**, B12304, doi:10.1029/2005JB003673, 2005.

Matsubara, M., K. Obara, and K. Kasahara, Three-dimensional P- and S-wave velocity structures beneath the Japan Islands obtained by high-density seismic stations by seismic tomography, *Tectonophysics*, **454**, 86–103, doi:10.1016/j.tecto.2008.04.016, 2008.

Matsubara, M., K. Obara, and K. Kasahara, High-Vp/Vs zone accompanying non-volcanic tremors and slow slip events beneath southwestern Japan, *Tectonophysics*, **472**, 6–17, doi:10.1016/j.tecto.2008.06.013, 2009.

Miura, S., S. Kodaira, A. Nakanishi, T. Tsuru, N. Takahashi, N. Hirata, and Y. Kaneda, Structural characteristics controlling the seismicity of southern Japan Trench fore-arc region, revealed by ocean bottom seismographic data, *Tectonophysics*, **363**, 79–102, 2003.

Miura, S., N. Takahashi, A. Nakanishi, T. Tsuru, S. Kodaira, and Y. Kaneda, Structural characteristics off Miyagi forearc region, the Japan Trench seismogenic zone, deduced from a wide-angle reflection and refraction study, *Tectonophysics*, **407**, 165–188, 2005.

Nakamichi, H., H. Watanabe, and T. Ohminato, Three-dimensional velocity structures of Mount Fuji and the South Fossa Magna, central Japan, *J. Geophys. Res.*, **112**, B03310, doi:10.1029/2005JB004161, 2007.

Nolet, G., *Seismic Tomography*, D. Reidel Publishing Company, 386 pp, 1987.

Okada, Y., K. Kasahara, S. Hori, K. Obara, S. Sekiguchi, H. Fujiwara, and A. Yamamoto, Recent progress of seismic observation networks in Japan—Hi-net, F-net, K-NET and KiK-net—, *Earth Planets Space*, **56**, xv–xxviii, 2004.

Sato, R., K. Abe, Y. Okada, K. Shimazaki, and Y. Suzuki, *Handbook of Earthquake Fault Parameters in Japan*, 390 pp., Kajima Shuppankai, Tokyo, 1989 (in Japanese)

Shao, G., X. Li, C. Ji, and T. Maeda, Preliminary result of the Mar 11, 2011 Mw 9.1 Honshu Earthquake, http://www.geol.ucsb.edu/faculty/ji/big_earthquakes/2011/03/0311/Honshu_main.html, 2011.

Shelly, D. R., G. C. Berzoa, H. Zhang, C. H. Thurber, and S. Ide, High-resolution subduction zone seismicity and velocity structure beneath Ibaraki Prefecture, Japan, *J. Geophys. Res.*, **111**, B06311, doi:10.1029/2005JB004081, 2006.

Takei, Y., Effect of pore geometry on VP/VS: from equilibrium geometry to crack, *J. Geophys. Res.*, **107**(B2), 2043, doi:10.1029/2001JB000522, 2002.

Ukawa, M., M. Ishida, S. Matsumura, and K. Kasahara, Hypocenter determination method of the Kanto-Tokai observational network for microearthquakes, *Res. Notes Natl. Res. Cent. Disaster Prev.*, **53**, 1–88, 1984 (in Japanese with English abstract).

Wessel, P. and W. H. F. Smith, New version of generic mapping tools released, *Eos Trans. AGU*, **79**, 329, 1995.

Yagi, Y., Coseismic slip model of Off the Pacific Coast of Tohoku earthquake, http://www.geol.tsukuba.ac.jp/ yagi-y/EQ/Tohoku/, 2011.

Yamazaki, T. and Y. Okamura, Subducting seamounts and deformation of overriding forearc wedges around Japan, *Tectonophysics*, **160**, 207–229, 1989.

Zhao, D., A. Hasegawa, and S. Horiuchi, Tomographic imaging of P and S wave velocity structure beneath northeastern Japan, *J. Geophys. Res.*, **97**, 19,909–19,928, 1992.

Zhao, D., Z. Wang, N. Umino, and A. Hasegawa, Tomographic imaging outside a seismic network application to the northeast Japan arc, *Bull. Seismol. Soc. Am.*, **97**, 1121–1132, 2007.

Zhao, D., M. Santosh, and A. Yamada, Dissecting large earthquakes in Japan: Role of arc magma and fluids, *Island Arc*, **19**, 4–16, 2010.

M. Matsubara (e-mail: mkmatsu@bosai.go.jp) and K. Obara